Computational Materials Science 179 (2020) 109683

Contents lists available at ScienceDirect

Computational Materials Science

journal homepage: www.elsevier.com/locate/commatsci

An atomistic simulation study investigating the effect of varying network structure and polarity in a moisture contaminated epoxy network

Rishabh Debraj Guha, Ogheneovo Idolor, Landon Grace*

North Carolina State University, USA

ARTICLE INFO

Keywords:
Epoxy
Crosslinking
Polarity
MAPS
Free-volume
Hydrogen bonding

ABSTRACT

Absorbed moisture is a frequent contributor to performance loss in polymer-based composite structures operating in nearly all environments. However, the fundamental mechanisms that govern water-polymer interaction remain poorly understood. In this molecular dynamics study, the polarity and internal structure of an epoxy-based composite matrix was varied through manipulation of crosslink density. A commonly used epoxy-hardener combination (DGEBA- DETA) was chosen and four different models were created with crosslinking density of 20%, 51%, 65% and 81% respectively. The results indicate that the increase in crosslinking leads to a greater availability of polar sites with a concomitant rise in available free volume. The rise in network polarity aids the hydrogen bonding interactions between the absorbed water and the composite matrix, but the greater availability of free volume also allows water molecules to cluster together through mutual hydrogen bonding activity. This results in a subsequent decrease in moisture interaction with polar sites at very high crosslink densities. It was also found that the diffusivity and average dipole moment of the absorbed moisture are correlated with the state of water molecules and that a greater percentage of network-bonded molecules tends to lower both of these quantities. These results are consistent with previously published experimental results which have contemplated the dual nature of water molecules in an epoxy network. The results also highlight the potential of leveraging this phenomenon for non-destructive inspection of the physical and chemical state of a polymer network.

1. Introduction

Epoxy-based polymer materials have become a critical component of many major engineering applications in both structural and non-structural roles. They find frequent use as encapsulants in the micro-electronic packaging industry [1,2] and have become an indispensable part of the automotive and aerospace sectors because of their ubiquitous use as a matrix material in polymer composites [3,4]. Epoxy based composite materials offer significant advantages over conventional materials because of their higher strength to weight ratio [5], resistance to chemical contamination [6], thermal stability and a low dielectric constant leading to better electrical insulation properties [7]. The low dielectric constant of epoxy-based composites is especially critical in radome applications, in which the radar signal must pass unimpeded through the protective radome structure [4].

Despite the numerous advantages associated with this class of materials, a major deterrent in their overall performance is their extreme sensitivity to moisture ingress [4,5,8,9]. Epoxies are known to absorb anywhere between 1 and 7% of moisture by weight [10]. Absorption of some degree is generally unavoidable; these materials readily absorb moisture when exposed to wet or humid environments and are frequently subjected to cycles of fluctuating temperature and humidity [3,11]. The absorbed moisture significantly impacts the performance of epoxy-based composite matrices by lowering glass-transition temperature (T_g) and degrading its thermal and electrical insulation properties. The electrical properties in particular are significantly degraded by the presence of water with its high relative permittivity. The extent of electrical property degradation is especially important in radome applications, where the volume, distribution, and state of absorbed water play critical roles in radar transmissivity and performance [4]. From a structural perspective, degradation of fiber–matrix interfaces [8], delamination [11], matrix swelling [12], and subsequent generation of micro cracks [5] have also been reported. Multiple studies have given evidence of matrix plasticization and degradation of the yield strength and overall mechanical properties of a composite due to moisture [3,11–15].

A thorough and fundamental understanding of the mechanism of transport, interaction behavior, and behavioral characteristics of moisture in an epoxy network is critical to actively mitigating the degradation of these material due to moisture ingress. In an attempt to

* Corresponding author at: Department of Mechanical and Aerospace Engineering, North Carolina State University, 911 Oval Drive, Raleigh, NC 27695, USA.
E-mail addresses: rdguha@ncsu.edu (R.D. Guha), oidolor@ncsu.edu (O. Idolor), landon_grace@ncsu.edu (L. Grace).

https://doi.org/10.1016/j.commatsci.2020.109683
Received 23 January 2020; Received in revised form 11 March 2020; Accepted 12 March 2020
Available online 19 March 2020
0927-0256/

elucidate the behavior of molecular water and its interactions in a polymer network, many experimental studies have been conducted using techniques like infra-red spectroscopy (NIR, FTIR), Nuclear Magnetic Resonance (NMR), and dielectric relaxation. Moy et al. [16] used broadline NMR spectroscopy to hypothesize the existence of water molecules bound to the polymer network at low moisture concentrations and secondary water molecules with greater mobility at higher moisture concentrations. Adamson et al. [17] explained the absorption phenomenon by attributing it to the free volume content in the epoxy. They suggested that water molecules first occupied the free volume "holes" in the network and were subsequently bound to the polar sites in the vicinity of the holes. Water sorption experiments in epoxy resins conducted by Apicella et al. [18] identified the presence of three different modes of sorption: (i) solution of water in the network, (ii) adsorption in holes which correspond to the excess free volume in the network and (iii) adsorption to the hydrophilic polar sites in the network which leads to polymer-water hydrogen bonding. However, a study by Jelinski et al. [19] which employed quadruple echo deuterium NMR spectroscopy refuted this hypothesis of the existence of "free" and "bound" water by concluding that water molecules hop from site to site in a polymer network with an approximate residence time per site of 7×10^{-10} s. Later dielectric relaxation studies by Pethrick et al. [20,21] were able to conclusively identify different states of water molecules in the network with distinct relaxation frequencies for the "bound" and "free" states. Herrera-Gómez et al. [22] and Musto et al. conducted gravimetric and FTIR spectroscopic studies [23–27] in the MIR and NIR range to bolster the theory of the dual nature of existence of water molecules in the polymer network.

A common takeaway from these studies is that there are multiple factors like free volume content, network polarity, and morphology which determine the characteristics of water behavior and diffusivity in an epoxy resin, but the conclusions are contradictory. According to Yu et al. [28], polarity is the primary factor which determines equilibrium moisture content while free volume content was instrumental in determining diffusivity. Mijovic et al. [29] conducted spectroscopic studies and concluded that 95% of water molecules reside near polar groups in epoxies and equilibrium water content is dependent on the number of available polar groups in the network. Conversely, Soles et al. [30,31] conducted a detailed study on multiple epoxy resins and established that as far as moisture-epoxy interactions are concerned, topology and polarity play a role in tandem with the locations of all the polar sites being coincident with the nanopores in the network. They concluded that the absolute zero hole volume had a strong correlation with the equilibrium moisture content and network polarity was the rate-limiting factor in moisture transport and diffusivity. Frank et al. [32] reached similar conclusions with regards to the diffusion coefficient after studying epoxy blends with different crosslink densities. They postulated that increasing crosslinking results in a greater number of polar sites in the network which, in turn, amplifies the tendency of the water molecules to become "bound" and contribute to slower diffusion rates. Multiple other studies [33–47] have tried to quantify this relationship between moisture and epoxy networks with differing characteristics, but a concrete understanding has still not been developed.

In light of the previous studies, it is clear that irrespective of the contradictory theories, the phenomenon which governs the interaction of moisture with an epoxy-amine system occurs at an atomistic scale. Hence a molecular level study will be very helpful in isolating the key factors and their respective roles in the moisture uptake characteristics of a polymer network. Molecular Dynamics (MD) simulation has been extensively used to study properties of a polymer system and its interactions with penetrant molecules. Yarovsky et al. [48] were among the first to model the crosslinking reaction in epoxy resins through MD simulations. Later, Wu et al. [49] and Varshney et al. [50] were able to develop more refined algorithms for simulating the crosslinking reaction using the Dreiding and CVFF forcefield, respectively. Among the many different studies on the structure and thermomechanical properties of such crosslinked networks [51–55], one article of particular interest is by Odegard et al. [52] which elucidated the effect of variation of crosslink density on properties like the glass-transition temperature (T_g), thermal expansion coefficients and elastic modulus.

MD simulations are very effective in quantifying non-bonded atomic interactions between different species. Thus, they have also been used to study the effect of moisture exposure and diffusing water molecules on an epoxy system [56–63]. Wu et al. [61] analyzed the effect of varying moisture concentration on properties like water diffusivity and fractional free volume in an epoxy network with a fixed degree of crosslinking. Mijovic et al. [57] conducted a molecular dynamics simulation to monitor the hydrogen bonds and the dynamics of water molecules in a fully cured epoxy network. Tam et al. [63] did similar work using the CVFF force field and bolstered previous results by quantifying H-bond formation probability at different moisture concentrations. In a recent work by our group [64] the correlation between secondary bonding interactions and the average dipole moment of the water molecules in a network was investigated. Although these studies provide critical information regarding the nature of interactions between water molecules and a polymer network, they do not isolate the role of network polarity. Despite the large volume of literature and relevant experimental work in the field, a dedicated simulation study which attempts to correlate the change in physical properties of a polymer network due to the molecular interactions between moisture and the polar sites is lacking.

In this study, we have modelled a commonly used commercial epoxy system comprised of Diglycidyl Ether of Bisphenol A (DGEBA) epoxy and Diethylene Tetra Amine (DETA) hardener to understand how the polar interactions between the network and absorbed water molecules change with varying crosslink density and, consequently, how that change manifests itself in the hydrogen bonding activity, diffusion behavior, and dipole moment fluctuations of the system. Through this work we aim to better understand the mechanism of moisture interaction in an epoxy matrix and the role of matrix polarity in influencing the nature and strength of these interactions.

2. Methods and simulation details

The two constituents of a polymer composite matrix - epoxy and the hardener - are in a highly crosslinked state which imparts the network with the necessary mechanical and thermal stability. In our case, an uncrosslinked system was modelled using the Amorphous Builder module in the MAPS platform of Scienomics (Materials and Processes Simulations Platform, Version 4.2.0, Scienomics SARL, Paris, France). The system consisted of the epoxy (DGEBA) and the hardener (DETA). The Crosslinker module in MAPS was used to generate systems with different crosslink densities and all MD simulations were executed using the open-source software package, LAMMPS [65]. The Amber Cornell Extension Force Field (ACEFF) which is a modified version of the Amber Cornell Force Field [66] was used to describe both the bonded and non-bonded interactions between atoms. The Gasteiger method [67], which is a type of electronegativity equalization method (EEM) was used to assign partial charges to each atom and for the water molecules the TIP3P model [68] was used. The crosslinker module is based on an algorithm similar to the one followed by Varshney et al. [50]. Subsequently, four different systems with varying crosslink densities were generated and each system was equilibrated. Post-equilibration, the systems were analyzed prior to moisture contamination and an effort was made to acquire the total free volume in the networks with different crosslink densities. This provides a preliminary understanding of how the increasing crosslinking would impact the volume occupied by voids in the network, which may have an impact on the nature of hydrogen bonding interactions. A fixed number of water molecules were then inserted into the four systems to obtain the desired degree of moisture contamination (by wt. %).

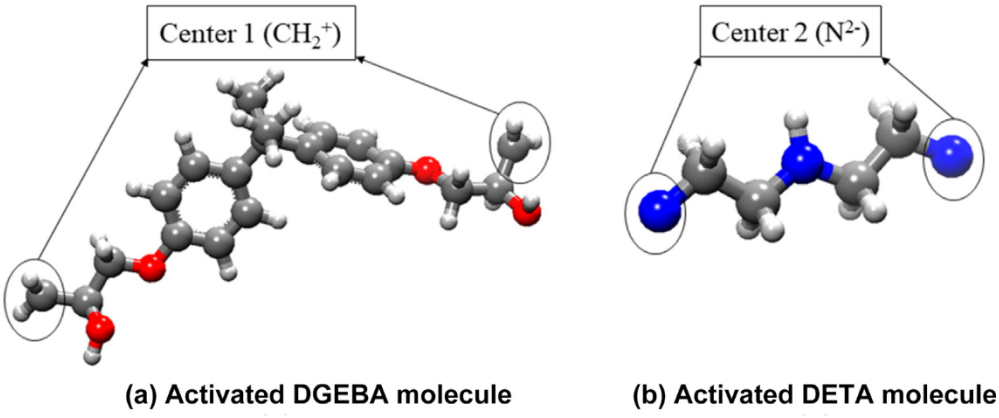

Fig. 1.

2.1. Crosslinking procedure

To execute the crosslinking reaction between the epoxy and the hardener molecules, 64 molecules of DGEBA and 32 molecules of DETA were first packed in a simulation cell. The activated DGEBA and DETA molecules used to construct the cell are shown in Fig. 1. The carbon, hydrogen, oxygen and nitrogen atoms have been represented by grey, white, red and blue colors respectively.

Care was taken to maintain the 2:1 ratio between the epoxy and the hardener molecules because an activated DGEBA molecule is bifunctional with two reaction sites (-CH^{2+}-) while the DETA molecule is tetrafunctional with four reaction sites (-N^{2-}-). Therefore, each molecule of DETA is capable of executing four crosslinking reactions while the DGEBA molecule can execute only two.

Each cycle in the crosslinking process consists of a geometry optimization (500 steps), a short NPT MD relaxation (5 picoseconds, 1000 steps) and then a 5-step algorithm which creates new bonds based on the distance between reaction centers. At the end of the cycle, if the target crosslinking percentage is achieved, the process is terminated. Using this iterative algorithm, four systems were obtained with crosslink densities of 20%, 51%, 65% and 81% respectively. During the crosslinking process, all the molecules involved (DGEBA/DETA) were in the activated state. This was necessary for the execution of the crosslinking reaction, but once the process was completed for a particular crosslinking density, the simulation cell was visualized in MAPS and all the reacted and the unreacted sites were selected. This can be done through the specific atom-group selection procedure in MAPS. Subsequently the unreacted CH_2^+ groups were located and a bond was created between CH_2^+ and the neighboring oxygen atom. Once all the bonds were formed, the hydrogens in the simulation cell was adjusted so that no atom in the cell was violating its valency. This led to the creation of crosslinked sites which had neighboring hydroxyl groups (from the crosslinking reaction procedure) and unreacted epoxy rings without any hydroxyl groups (from the bond creation process). The geometry optimization process (described later) was performed after this so that the structure can be relaxed to its equilibrium state. This also led to the optimization of bond lengths in the manually created bonds in the epoxy rings. Because greater crosslinking generates a larger number of polar hydroxyl sites, the first network with the lowest crosslink density was the least polar in nature while the final network obtained had the highest polarity.

2.2. Simulations prior to moisture contamination

After the four systems of varying crosslink densities were obtained, their energies were minimized through a 500-step geometry optimization using the Steepest Descent method. In experimental conditions, the curing reaction between epoxy and hardener molecules is performed at elevated temperatures and the reaction products are slowly cooled to a lower temperature in a post-cure process. Similarly, in the crosslinker module, the simulation temperatures are high and it is critical to slowly lower the temperature and equilibrate the cell at that temperature before introducing moisture contamination. A large gradient in temperature in a single simulation will not produce a stable and well-equilibrated cell, especially if the simulation time period is not sufficiently long. Therefore, a multi-step anneal and equilibrate method was followed to sequentially lower the temperature and keep the simulation cell equilibrated. In this method, the temperature of the cell was lowered from 600 K to 300 K in six steps. The periodic boundary conditions were imposed on each simulation cell. In each step, the temperature was reduced by 50 K through a 100 picosecond (ps) MD simulation using the constant pressure and temperature (NPT) ensemble. After the 100 ps simulation was completed, the cell was equilibrated at that temperature using a short 20 ps NPT simulation. The NPT ensemble was selected because it allowed the pressure to be kept fixed at 1 atm during the simulation time period; an approximate replication of the actual experimental scenario. In all simulations, the Nose-Hoover barostat with a damping of 350 fs (fs) and thermostat with a damping of 10 fs were used to control temperature and pressure in the ensemble. The cut-off distance for non-bonded interactions was set at 12 Å and the particle-mesh method with an accuracy of 0.0001 was used to calculate the summation of the electrostatic forces.

As seen in Fig. 2a, the total energy of the system decreased with temperature during the 100 ps simulation. In the same simulation period, there was a gradual but steady rise in the system density – indicating that the volume of the system decreased as the system relaxed. During the short, fixed-temperature equilibration run the total energy fluctuated about a mean, as seen in Fig. 2b. A short simulation period of 20 ps which was used for the final equilibration cycle at 300 K was not sufficient to obtain a conclusive estimate of the accessible free volume in the system. Therefore, the four systems were further equilibrated for a longer time period of 1 ns (1000 ps) at the final equilibration temperature (300 K).

2.3. Simulations on moisture contaminated cells

The Amorphous Builder module in MAPS was employed to randomly insert 50 water molecules (corresponding to a moisture contamination of approximately 3.5% by wt.) in the well-equilibrated crosslinked systems. Fig. 3(a) and (b) show a dry crosslinked system and a moisture contaminated crosslinked system respectively. A detailed view of one of the unreacted epoxy rings and a crosslinked site in a dry simulation cell is also shown in the middle of Fig. 3.

Epoxy resins generally absorb anywhere between 3 and 4% of moisture in the linear region of the absorption curve [17]. For every system with a particular crosslink density, four representative systems

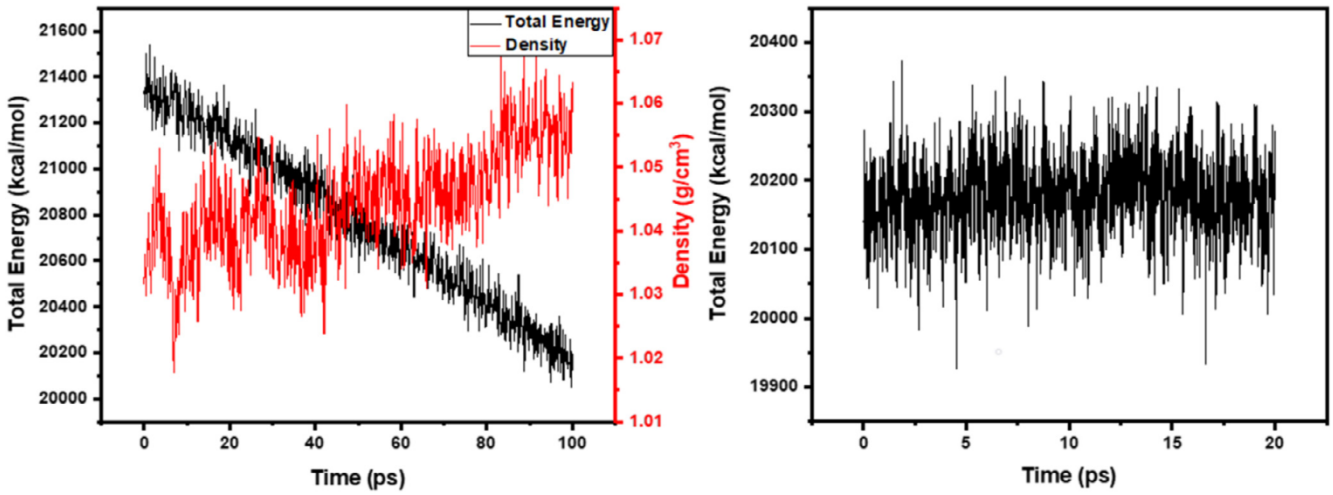

Fig. 2. Evolution of - a) Total energy and density in an annealing cycle b.) Total energy in subsequent equilibration cycle.

were created by randomly perturbing the water molecules in the system. This resulted in 16 different simulation systems; 4 different crosslink densities and 4 representative systems for each crosslink density. The creation of multiple systems for a single crosslink density allowed us to take an average over four different systems and reduce the probability of an outlier.

Once moisture was introduced in the system, a 500-step geometry optimization was performed on each system using the Steepest Descent method as described previously. Post-optimization, the systems were subjected to a long NPT simulation of 5 ns (5000 ps). It was imperative to allow sufficient time for the water molecules to navigate the entire polymer network. Hence, a long simulation time period was chosen to permit an accurate estimation of the hydrogen bonds formed by the polar molecules after proper equilibration.

The H-O bond length and the H—O—H bond angle was kept fixed using the 'fix-shake' command in LAMMPS because water molecules have a fixed bond length and bond angle of 0.96 Å and 104.5°, respectively [69]. Allowing the bond length or angles to vary during the simulation would produce unphysical results.

3. Results and discussion

3.1. Mechanical properties

Before exploring the nature of interactions between the water molecules and the network, it was critical to validate the equilibrated models with different crosslink densities prior to moisture contamination. For this purpose, the mechanical properties of the dry crosslinked cells obtained from our simulations were compared with the results from the literature in which thermomechanical properties of a crosslinked epoxy resin were evaluated through MD simulations.

To calculate the Young's modulus for our epoxy models, a constant stress method was employed. A 1 ns (1000 ps) NPT simulation was conducted on the equilibrated systems. During the simulation period a constant stress of 1000 atm was applied in the x-direction. To prevent the simulation from becoming unstable, the applied stress must be carefully selected. The shear rate produced in the system due to the stress should be small enough for it to deform in the direction of the force. In general, a stress rate of 1 atm/ps is appropriate. Once the simulation was complete, a Python post-processing script was used to calculate the Young's modulus from the linear region of the stress–-strain curve. As seen in Fig. 4, at low crosslink densities of 20% the Young's modulus is very low (~0.3 GPa). As the crosslink density

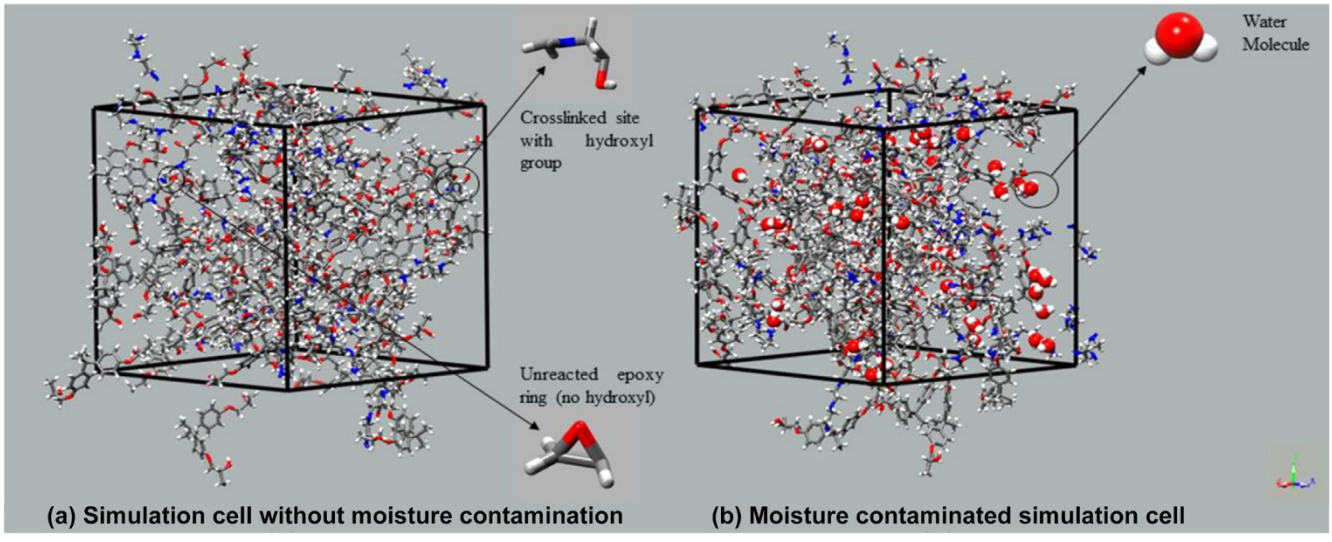

Fig. 3.

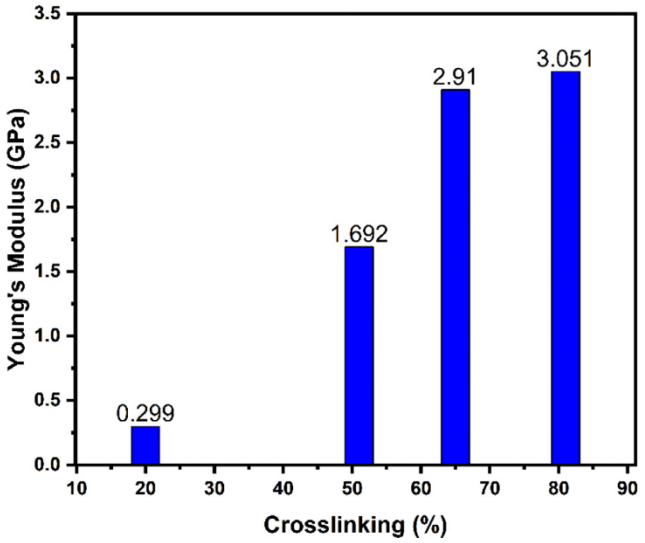

Fig. 4. Mechanical Properties at different crosslink densities.

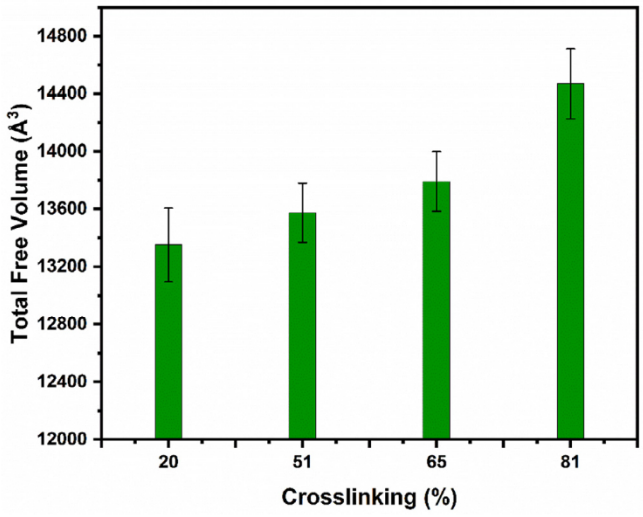

Fig. 5. Variation of total free volume with increasing crosslink density.

increases, the Young's modulus of the epoxy network likewise increases. This trend is consistent with known behavior; greater crosslink density results in a higher number of covalent bonds in the network, which results in improved strength and better mechanical properties. Another interesting observation is that there is no significant improvement in Young's Modulus when the crosslink density increases from 65% to 81%. This might indicate diminishing gains in increased stiffness with an increasing degree of crosslinking beyond 80%. This trend is consistent with the results of Odegard et al. [52] where the mechanical properties plateaued when the crosslink density increased from 63% to 76%.

An experimental study conducted by Littell et al. [70] on a fully cured DGEBF/DETDA resin at different strain rates in both tension and compression yielded values for Young's modulus in the range of 1.66–2.89 GPa, (consistent with the values derived from this simulation). Multiple MD studies have been performed on different epoxy systems with a variety of forcefields. The results of these studies are summarized in Table 1 and are consistent with the values obtained in our simulations. Based on the agreement between the simulations and results reported in the literature, it is reasonable to assume that the equilibrated models obtained in our simulations were valid and can be used to study the effect of moisture contamination.

3.2. Free volume evolution

The moisture uptake in any epoxy network is correlated with the amount of fractional free volume available in the system [32]. As mentioned in the works of Soles et al. [30,31], the equilibrium moisture uptake in an epoxy resin is dictated primarily by two factors: the volume occupied by nanopores at absolute zero (V_o) and the overall polarity of the network. With respect to the latter, the role of polarity will be explored in subsequent sections through the investigation of secondary bonding between water and the polar sites in the network. With respect to the former, the free volume of the system was evaluated at different crosslink densities prior to contaminating the epoxy networks with moisture. This was done by executing an additional NPT simulation of 1 ns at 300 K after the final equilibration cycle was completed.

The analyzer was then used to calculate the free volume at every picosecond over this simulation period of 1 ns (1000 ps) and a total average free volume was calculated between 200 ps and 1000 ps which gave a measure of the fractional volume occupied by voids and nanopores in the network. The first 200 ps was neglected to allow the system to fully equilibrate and neglect any transitional states in the system. As observed in Fig. 5, the total free volume increased as the crosslink density increased – indicating greater availability for water molecules in the system. The same trend was seen when the free volume available for spherical probes of different radii was evaluated as seen in Table 2. This was consistent with previous experimental results [30,32] and the MD results obtained by Strachan et al. [71] and Zhang et al. [72]. The behavior can be explained by the directional nature of covalent bonds. As crosslink density increases, the number of covalent bonds formed between the epoxy and the hardener molecules also increase. Due to the directional nature of the newly formed bonds, their bond length and angles are fixed, which reduces the molecular degrees of freedom. The lack of mobility in the network leads to a lower packing efficiency and hence a greater fraction of free volume.

3.3. H-bonding activity

The state of water molecules and their mobility in an epoxy network is primarily dictated by the type of H-bonds formed by the molecules and their respective concentrations. In an epoxy network there are multiple polar sites which are partially charged due to the electronegativity differences between the participating atoms in a covalent bond of the network. Additionally, water itself is a highly polar molecule due to the large electronegativity difference between hydrogen and oxygen. Table 3 summarizes the different polar species in the epoxy-

Table 1
Comparison of mechanical properties with previous results.

	Epoxy/Hardener	Crosslinking	E(GPa)
Arab [51]	DGEBA/DETA	0%-81%	2.8–3.8
Beni [52]	DGEBA/DETA	50%	~2.8
Strachan [53]	DGEBF/DETDA	78%	3.2–3.5
Odegard [54]	DGEBF/DETDA	54–76%	0.4–2.3
Masoumi [55]	DGEBA/D-230	0–100%	2.6–3.9
Current study	**DGEBA/DETA**	**20–81%**	**0.3–3.1**

Table 2
Comparison of accessible free volume using spherical probes of different radii.

Crosslink density	Free volume (r = 1 Å)	Free volume (r = 1.5 Å)	Total free volume (no probe)
20%	226.67 Å^3	8.87 Å^3	13351.17 Å^3
51%	341.43 Å^3	17.72 Å^3	13573.79 Å^3
65%	505.80 Å^3	49.99 Å^3	13791.91 Å^3
81%	762.82 Å^3	101.24 Å^3	14469.68 Å^3

Table 3
Partial charges assigned to all polar atoms in polymer network.

Polar species	Description	Partial charge
Ow	Oxygen in water molecule	−0.8300
Hw	Hydrogen in water molecule	+0.4150
OH	Oxygen in Hydroxyl group of epoxy	−0.3882
HO	Hydrogen in Hydroxyl group of epoxy	0.2099
Oe	Oxygen in Ether group of epoxy	−0.3421
Ou	Oxygen in unreacted ring of epoxy	−0.3694
N1	Primary Nitrogen atom in hardener	−0.3283
H1	Hydrogen atom connected to Primary Nitrogen	+0.1183
N2	Secondary Nitrogen atom in hardener	−0.3136
H2	Hydrogen atom connected to Secondary Nitrogen	+0.1220
N3	Tertiary Nitrogen atom in hardener	−0.2961

water system of our study and the respective partial charges assigned to them. All the polar species which have a partial negative charge are potential acceptors while the hydrogen atoms with a partial positive charge are donors. In our study, the H-bond was calculated based on a geometric criterion, i.e. if the distance and the angle between a donor-acceptor pair was found to be below a certain threshold, then it was assumed that a H-bond was present at that site. We used a Python script in MAPS for counting the number of H-bonds with a cut-off distance of 2.5 Å and a cut-off angle of 90° [72]. For a selected group of atoms, the H-bonds were counted over the entire simulation period of 5 ns (5000 ps) and then an average value was calculated over the last 1 ns of the simulation time frame. This was done to ensure that the H-bond values are calculated only after the system has been well equilibrated. As discussed earlier, this procedure was repeated for all four simulated systems created at a particular crosslink density and the average value of the four systems was considered for any further analysis.

Before exploring the relationship between crosslinking density and secondary bonding interactions between water and the network, the H-bonding activity within the polar sites of the network was investigated. In our epoxy system the carbon atoms in the network had negligible charge ($< \pm 0.1$) and were considered non-polar. As seen in Fig. 6, the average number of H-bonds formed by the polar sites in the network increased with increasing crosslinking, which is a direct result of the increased number of hydroxyl groups in networks with higher crosslink densities. A greater number of hydroxyl groups would lead to a higher number of HO sites which can act as donors for forming an H-bond with the other polar acceptor groups (like N1/N2/N3, OH, Oe and Ou).

The first step in understanding the nature of interactions between moisture and the network is to understand the different types of H-bond a water molecule can form within the network. A random water molecule in the polymer network can form a hydrogen bond with another water molecule. In this scenario, the oxygen atom of one water molecule (Ow) will act as an acceptor while the hydrogen atom of another water molecule will be the donor (Hw) and these H-bonds are denoted as Type-I H-bonds. The water molecule can also form an H-bond with the polar atoms in the polymer network - denoted as Type-II H-bonds. This nomenclature is consistent with our previous work [64]. The calculation of the Type-I H-bonds was straightforward, with the script calculating the number of H-bonds only over the selected water molecules.

For calculating the number of Type-II H-bonds, the following approach was chosen. First, the total number of H-bonds in the system was calculated, i.e., all the polar species in the system were selected including the water molecules. The number of H-bonds formed by polar sites in the network (Fig. 6) and the Type-I H-bonds formed by the water molecules were then subtracted from the total number of H-bonds formed. This gave a measure of the number of H-bonds formed between the water molecules and the polar sites in the network.

The variation in the number of Type-I and Type-II H-bonds with increasing crosslinking is shown in Fig. 7. The increase in crosslink density has opposing effects on the trends followed by the Type-I and Type-II H-bonds. We can observe that an initial increase in crosslink density is associated with a rise in the concentration of Type-II H-bonds, while the Type-I H-bonds in the system decrease. However, as the crosslink density further increases, the trend reverses and the concentration of Type-II H-bonds gradually falls with a simultaneous increase in the number of Type-I H-bonds.

It has been mentioned in multiple previous studies [10,30–32,36] that the nature of interaction between the epoxy and the water molecules entrapped within the network is dictated not only by the polarity of the network but also by the free volume available within the network. In the epoxy systems simulated in this study, as the crosslink density of the system increases from 20% to 51%, the polarity of the system increases with a greater availability of polar sites for the water molecules to participate in a Type-II H-bond. As the number of water molecules present in all the systems is the same, this results in a drop in the average number of Type-I H-bonds in the system. But as the crosslink density further increases, the rise in polarity is also accompanied by a rise in total free volume in the system as seen in Fig. 5. These two effects of increasing polarity and free volume are in competition regarding the formation of one type of H-bond over the other. The greater polarity drives the water molecules to participate in a Type-

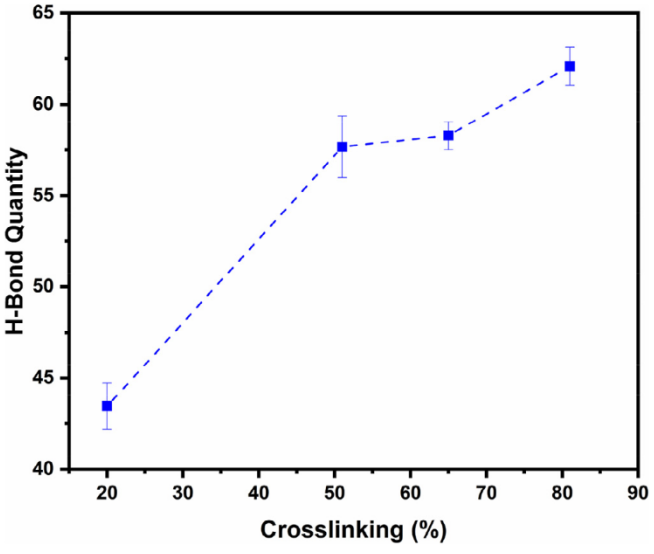

Fig. 6. Variation of H-bonds formed between polar sites in the network.

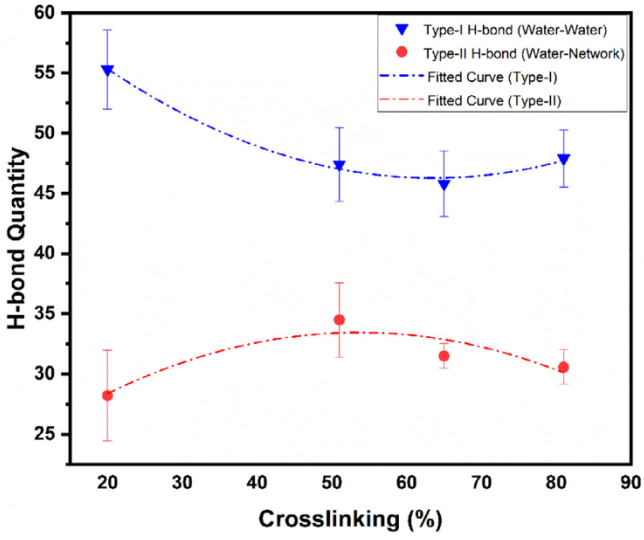

Fig. 7. Types of H-bonds formed by water molecules and their variation with increasing crosslink density.

II H-bond, while the increased free volume provides opportunities for the water molecular to form clusters (Type-I H-bonds). We hypothesize that the trend observed in Fig. 7 is due to the combination of these two effects with the rise in polarity dominating in the initial increase of crosslink density and the rise in free volume having a more pronounced influence at higher crosslink densities.

3.4. Mean squared displacement (MSD) and diffusion coefficient

The diffusion coefficient (D) of the water molecules in the different epoxy systems with varying crosslink densities provides an estimate of the mobility of moisture in the individual networks. In MD simulations, D can be calculated from the mean square displacement (MSD) curves of the water molecules during the simulation time period. The MSD of thermally-excited water molecules can be defined as its trajectory with time as it randomly traverses the polymer matrix [56] and is given by Eq. (1) :-

$$MSD(t - t_0) = \frac{1}{6N}\sum_{i=1}^{N}(r_i(t) - r_i(t_0))^2 \quad (1)$$

where $r_i(t)$ is the position of the ith water molecule at time t. The diffusion coefficient can be estimated from the MSD curve by finding the slope in the initial linear region [58,73] as shown in Eq. (2):-

$$D = \lim_{t\to\infty}\frac{d}{dt}MSD(t - t_0) \approx \langle\frac{d}{dt}MSD(t - t_0)\rangle_{t_1}^{t_2} \quad (2)$$

The initial part of the MSD curves is generally neglected because these regions are mostly non-linear. Fig. 8 shows the MSD curves for the water molecules in one of the models at different crosslink densities. As inferred from the Figure, the best time period where all the four curves are reasonably linear is between 500 and 1000 ps and this window was chosen for applying Eq. (2) to calculate D.

It is observed in Fig. 9 that the diffusion coefficient is correlated with the state of water molecules in the system. At lower crosslink densities, when the polarity of the system is low and the water molecules have a higher tendency to form Type-I H-bonds, the diffusion coefficient (D) is comparatively high. But as the polarity of the system increases with crosslinking, the water molecules start forming Type-II H-bonds resulting in lower diffusion coefficients. This is consistent with previous results [32] where it was postulated that the tendency of water molecules to become “bound” to polar sites may contribute to slower diffusion rates in epoxies with higher crosslink densities. When a random water molecule is traversing in a polymer network with high

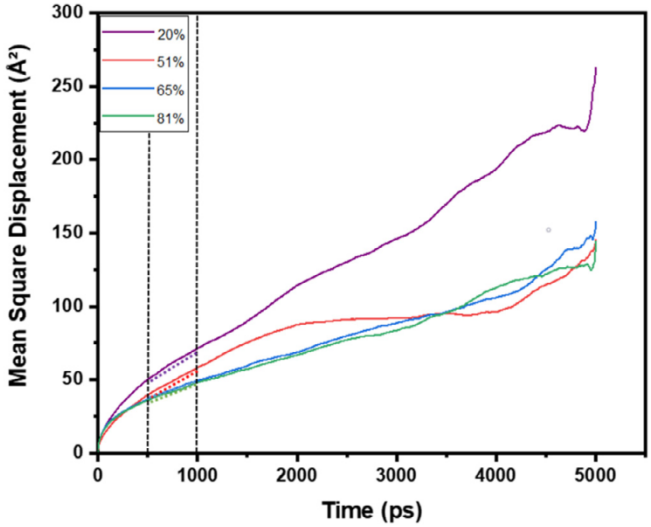

Fig. 8. MSD curves for water molecules (Model-1) with increasing crosslink densities.

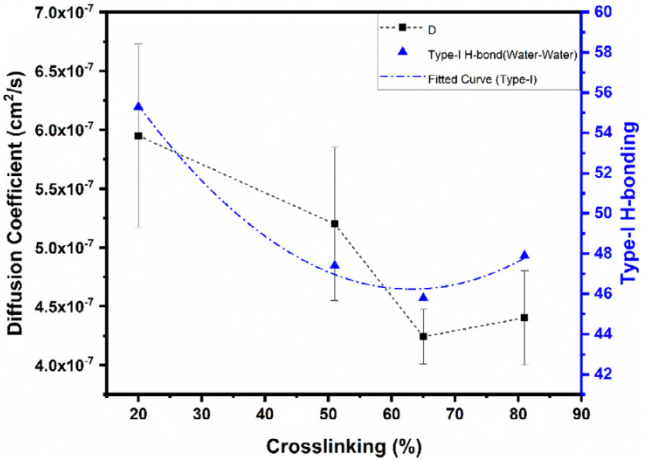

Fig. 9. Correlation between diffusion coefficient and Type-I H-bonds at different crosslink densities.

crosslink density, there is a greater probability for it to encounter a polar site, which impedes the molecule’s mobility. As discussed in the previous section, at very high crosslink densities the higher free volume in the network aids the clustering of water molecules and increases the number of Type-I H-bonds, which manifests in the gradual rise of the diffusion coefficient from 65% to 81%.

3.5. Average dipole moment fluctuations

The static dielectric constant has a strong correlation with the total dipole moment of the system. This has previously been explored in MD simulations to estimate static permittivity [74,75]. For our study, we attempted to understand the influence of the increasing polarity on the dipole moment fluctuations of the epoxy systems. Under the application of an electromagnetic field, the water molecules which are bound at the polar sites will have restricted dipolar rotations due to its secondary interactions with the network. These water molecules will have a lower dipole moment when compared to bulk water molecules in the system with negligible interactions with the epoxy. If the moisture concentration is kept constant across the systems, then the increasing polarity should have an impact on the average dipole moment of the water molecules.

To investigate this phenomenon, the dipole moment fluctuations of the water molecules in all four moisture-contaminated systems over the simulation period of 5 ns were evaluated using the MAPS analyzer and an average dipole moment was calculated over the simulation period. As seen in Fig. 10, there is a decreasing trend in the dipole moment fluctuations averaged over four models at a particular crosslink density. This supports the hypothesis that the increasing polarity of the epoxy networks leads to a greater tendency of the water molecules to engage in H-bonding with the polar sites in the network (Type-II H-bond). As the moisture concentration across all systems was held constant, the number of water molecules that had dipolar characteristics similar to bulk water decreased and the average dipole moment of the water molecules in the system went down. These results also suggest that water molecules in moisture contaminated composites which are not residing in micro-cracks and voids will have suppressed dipolar rotation as highly crosslinked matrices are used almost exclusively in polymer-based composites.

4. Conclusions

The nature of interactions between an epoxy system and ingressed moisture molecules is complex and depends on multiple factors like cure temperature, network structure, chemical constituents, ambient

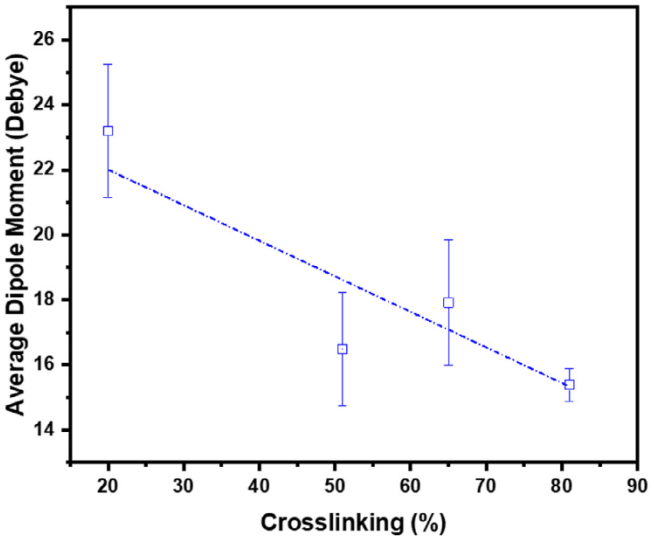

Fig. 10. Variation of average dipole moment with increasing crosslink density.

conditions, and exposure time. In this study, an attempt was made to isolate the role of network structure and polarity on the molecular interactions between moisture and polar sites in an epoxy network. We were able to conclude that both the free volume and the network polarity play a critical role in determining the H-bonding state of a random water molecule in an epoxy network. The increase in free volume (13351.17–14469.68 $Å^3$) and network polarity with the increasing crosslink density (20–80%) suggests that the type and number of H-bonds formed were dependent on both these factors. The increase in free volume promoted the clustering of water molecules and an increase in the number of Type-I H-bonds, while the increase in network polarity aided the formation of Type-II H-bonds. These effects on the hydrogen-bonded state of the water molecules also had a bearing on physical properties like the diffusion coefficient and the average dipole moment fluctuations, with the former having a correlation with the Type-I H-bonds formed by the water molecules and the latter having a decreasing trend with increasing polarity.

The findings also have direct implications for practical applications of epoxy resins, which are common among polymer-based composites. In particular, the state of the absorbed water molecules and the resulting dielectric behavior, which is directly correlated with the polarity of the network, has substantial implications for electrical applications such as composite radomes or other structures which require a low dielectric constant. While other material properties (such as hydrophobicity) may ultimately govern the design and composition of a radome, an epoxy matrix with greater polarity may be preferable due to its ability to restrict dipolar rotation of absorbed moisture and maintain high radar transmissivity in the presence of absorbed moisture.

The difference in the nature of secondary interactions of the water molecules with the network depending on free volume also has practical implications. The results show that increasing free volume has an impact on these interactions. Thus, physical damage that generates new free volume through micro-cracks and voids is likely to influence the dielectric behavior of the bulk composite due to the altered interaction between moisture and the polymer network in damaged areas. This phenomena may be useful in non-destructive detection of damaged areas through experimental methods like infrared spectroscopy and dielectric resonance.

CRediT authorship contribution statement

Rishabh Debraj Guha: Conceptualization, Methodology, Software, Data curation, Visualization, Writing - original draft. **Ogheneovo Idolor:** Conceptualization, Resources, Writing - review & editing. **Landon Grace:** Supervision, Project administration, Funding acquisition, Writing - review & editing.

Declaration of Competing Interest

The authors declare that they have no known competing financial interests or personal relationships that could have appeared to influence the work reported in this paper.

Acknowledgement

This material is based upon work partially supported by the National Science Foundation (NSF) - US. under Grant Number: CMMI-175482. The authors would like to acknowledge the support and insight of Dr. Melissa Pasquinelli (College of Natural Resources (NCSU)) and the HPC cluster at NCSU for allotting us the computational time for running our simulations.

Data Availability

The raw/processed data required to reproduce these findings cannot be shared at this time as the data also forms part of an ongoing study.

Appendix A. Supplementary data

Supplementary data to this article can be found online at https://doi.org/10.1016/j.commatsci.2020.109683.

References

[1] B. Wunderle, E. Dermitzaki, O. Holck, et al., Molecular dynamics simulation and mechanical characterisation for the establishment of structure-property correlations for epoxy resins in microelectronics packaging applications, Mechanical and Multi-Physics Simulation and Experiments in Microelectronics and Microsystems, IEEE, 2009, pp. 1–11.
[2] L. Garden, R.A. Pethrick, A dielectric study of water uptake in epoxy resin systems, J. Appl. Polym. Sci. 134 (2017).
[3] F.R. Jones, J.P. Foreman, The response of aerospace composites to temperature and humidity, Polymer Composites in the Aerospace Industry, Elsevier, 2015, pp. 335–369.
[4] L.R. Grace, The effect of moisture contamination on the relative permittivity of polymeric composite radar-protecting structures at X-band, Compos. Struct. 128 (2015) 305–312.
[5] F. Ellyin, C. Rohrbacher, The influence of aqueous environment, temperature and cyclic loading on glass-fibre/epoxy composite laminates, J. Reinf. Plast. Compos. 22 (2003) 615–636.
[6] B. Dębska, L. Lichołai, Resin composites with high chemical resistance for application in civil engineering, Period. Polytech. Civil Eng. 60 (2016) 281–287.
[7] J. Seo, W. Jang, H. Han, Thermal properties and water sorption behaviors of epoxy and bismaleimide composites, Macromol. Res. 15 (2007) 10–16.
[8] C.L. Schutte, Environmental durability of glass-fiber composites, Mater. Sci. Eng. R Rep. 13 (1994) 265–323.
[9] Idolor O., R. Guha & L. Grace. 2018. A Dielectric Resonant Cavity Method for Monitoring of Damage Progression in Moisture-Contaminated Composites. American Society for Composites 2018.
[10] C.L. Soles, A.F. Yee, A discussion of the molecular mechanisms of moisture transport in epoxy resins, J. Polym. Sci., Part B: Polym. Phys. 38 (2000) 792–802.
[11] H.N. Dhakal, Z. Zhang, Polymer matrix composites: moisture effects and dimensional stability, Wiley Encycl. Compos. (2011) 1–7.
[12] P.S. Theocaris, E.A. Kontou, G.C. Papanicolaou, The effect of moisture absorption on the thermomechanical properties of particulates, Colloid Polym. Sci. 261 (1983) 394–403.
[13] T.S. Ellis, F.E. Karasz, Interaction of epoxy resins with water: the depression of glass transition temperature, Polymer 25 (1984) 664–669.
[14] L.R. Grace, M.C. Altan, Characterization of anisotropic moisture absorption in polymeric composites using hindered diffusion model, Compos. A Appl. Sci. Manuf. 43 (2012) 1187–1196.
[15] L.R. Grace, M.C. Altan, Non-fickian three-dimensional hindered moisture absorption in polymeric composites: model development and validation, Polym. Compos. 34 (2013) 1144–1157.
[16] P. Moy, F.E. Karasz, Epoxy-water interactions, Polym. Eng. Sci. 20 (1980) 315–319.
[17] M.J. Adamson, Thermal expansion and swelling of cured epoxy resin used in graphite/epoxy composite materials, J. Mater. Sci. 15 (1980) 1736–1745.
[18] A. Apicella, R. Tessieri, C. de Cataldis, Sorption modes of water in glassy epoxies, J. Membr. Sci. 18 (1984) 211–225.
[19] L.W. Jelinski, J.J. Dumais, A.L. Cholli, et al., Nature of the water-epoxy interaction,

Macromolecules 18 (1985) 1091–1095.
[20] R.A. Pethrick, E.A. Hollins, I. McEwan, et al., Dielectric, mechanical and structural, and water absorption properties of a thermoplastic-modified epoxy resin: poly (ether sulfone) − amine cured epoxy resin, Macromolecules 29 (1996) 5208–5214.
[21] D. Hayward, E. Hollins, P. Johncock, et al., The cure and diffusion of water in halogen containing epoxy/amine thermosets, Polymer 38 (1997) 1151–1168.
[22] A. Herrera-Gómez, G. Velázquez-Cruz, M.O. Martín-Polo, Analysis of the water bound to a polymer matrix by infrared spectroscopy, J. Appl. Phys. 89 (2001) 5431–5437.
[23] S. Cotugno, G. Mensitieri, P. Musto, et al., Molecular interactions in and transport properties of densely cross-linked networks: a time-resolved FT-IR spectroscopy investigation of the epoxy/H2O system, Macromolecules 38 (2005) 801–811.
[24] P. Musto, L. Mascia, G. Ragosta, et al., The transport of water in a tetrafunctional epoxy resin by near-infrared Fourier transform spectroscopy, Polymer 41 (2000) 565–574.
[25] P. Musto, G. Ragosta, L. Mascia, Vibrational spectroscopy evidence for the dual nature of water sorbed into epoxy resins, Chem. Mater. 12 (2000) 1331–1341.
[26] P. Musto, G. Ragosta, G. Scarinzi, et al., Probing the molecular interactions in the diffusion of water through epoxy and epoxy–bismaleimide networks, J. Polym. Sci. Part B Polym. Phys. 40 (2002) 922–938.
[27] S. Cotugno, D. Larobina, G. Mensitieri, et al., A novel spectroscopic approach to investigate transport processes in polymers: the case of water–epoxy system, Polymer 42 (2001) 6431–6438.
[28] S. Li, L. Li, Y. Yu, et al., Effect of chemical structure on the water sorption of amine-cured epoxy resins, Corros. Sci. 51 (2009) 3000–3006.
[29] J. Mijović, H. Zhang, Local dynamics and molecular origin of polymer network − Water interactions as studied by broadband dielectric relaxation spectroscopy, FTIR, and molecular simulations, Macromolecules 36 (2003) 1279–1288.
[30] C.L. Soles, F.T. Chang, D.W. Gidley, et al., Contributions of the nanovoid structure to the kinetics of moisture transport in epoxy resins, J. Polym. Sci. Part B Polym. Phys. 38 (2000) 776–791.
[31] C.L. Soles, F.T. Chang, B.A. Bolan, et al., Contributions of the nanovoid structure to the moisture absorption properties of epoxy resins, J. Polym. Sci. Part B Polym. Phys. 36 (1998) 3035–3048.
[32] K. Frank, C. Childers, D. Dutta, et al., Fluid uptake behavior of multifunctional epoxy blends, Polymer 54 (2013) 403–410.
[33] M.K. Antoon, J.L. Koenig, T. Serafini, Fourier-transform infrared study of the reversible interaction of water and a crosslinked epoxy matrix, J. Polym. Sci. Polym. Phys. Ed. 19 (1981) 1567–1575.
[34] V. Bellenger, J. Verdu, E. Morel, Structure-properties relationships for densely cross-linked epoxide-amine systems based on epoxide or amine mixtures, J. Mater. Sci. 24 (1989) 63–68.
[35] Enns J. B. & J. K. Gillham. 1983. Effect of the Extent of Cure on the Modulus, Glass Transition, Water Absorption, and Density of an Amine-Cured Epoxy.
[36] K. Frank, J. Wiggins, Effect of stoichiometry and cure prescription on fluid ingress in epoxy networks, J. Appl. Polym. Sci. 130 (2013) 264–276.
[37] C. Grave, I. McEwan, R.A. Pethrick, Influence of stoichiometric ratio on water absorption in epoxy resins, J. Appl. Polym. Sci. 69 (1998) 2369–2376.
[38] J.L. Halary, Structure-property relationships in epoxy-amine networks of well-controlled architecture, High Perform. Polym. 12 (2000) 141–153.
[39] M. Jackson, M. Kaushik, S. Nazarenko, et al., Effect of free volume hole-size on fluid ingress of glassy epoxy networks, Polymer 52 (2011) 4528–4535.
[40] L. Li, Y. Yu, H. Su, et al., The diffusion mechanism of water transport in amine-cured epoxy networks, Appl. Spectrosc. 64 (2010) 458–465.
[41] L. Li, S. Zhang, Y. Chen, et al., Water transportation in epoxy resin, Chem. Mater. 17 (2005) 839–845.
[42] C. Maggana, P. Pissis, Water sorption and diffusion studies in an epoxy resin system, J. Polym. Sci. Part B Polym. Phys. 37 (1999) 1165–1182.
[43] I. Merdas, F. Thominette, A. Tcharkhtchi, et al., Factors governing water absorption by composite matrices, Compos. Sci. Technol. 62 (2002) 487–492.
[44] P. Nogueira, C. Ramírez, A. Torres, et al., Effect of water sorption on the structure and mechanical properties of an epoxy resin system, J. Appl. Polym. Sci. 80 (2001) 71–80.
[45] J. Wang, B. Wang, J. Gong, et al., Effect of curing agent polarity on water absorption and free volume in epoxy resin studied by PALS. Nuclear Inst. Methods Phys. Res. B 268 (2010) 2355–2361.
[46] H. Wang, Y. Liu, J. Zhang, et al., Effect of curing conversion on the water sorption, corrosion resistance and thermo-mechanical properties of epoxy resin, RSC Adv. 5 (2015) 11358.
[47] C. Hoeve, The structure of water in polymers, Water Polym. (1980) 135–146.
[48] I. Yarovsky, E. Evans, Computer simulation of structure and properties of cross-linked polymers: application to epoxy resins, Polymer 43 (2002) 963–969.
[49] C. Wu, W. Xu, Atomistic molecular modelling of crosslinked epoxy resin, Polymer 47 (2006) 6004–6009.
[50] V. Varshney, S.S. Patnaik, A.K. Roy, et al., A molecular dynamics study of epoxy-based networks: cross-linking procedure and prediction of molecular and material properties, Macromolecules 41 (2008) 6837–6842.
[51] C. Li, A. Strachan, Molecular simulations of crosslinking process of thermosetting polymers, Polymer 51 (2010) 6058–6070.
[52] A. Bandyopadhyay, P.K. Valavala, T.C. Clancy, et al., Molecular modeling of crosslinked epoxy polymers: the effect of crosslink density on thermomechanical properties, Polymer 52 (2011) 2445–2452.
[53] S. Masoumi, B. Arab, H. Valipour, A study of thermo-mechanical properties of the cross-linked epoxy: an atomistic simulation, Polymer 70 (2015) 351–360.
[54] A. Shokuhfar, B. Arab, The effect of cross linking density on the mechanical properties and structure of the epoxy polymers: molecular dynamics simulation, J. Mol. Model. 19 (2013) 3719–3731.
[55] F. Aghadavoudi, H. Golestanian, Y. Tadi Beni, Investigating the effects of resin crosslinking ratio on mechanical properties of epoxy-based nanocomposites using molecular dynamics, Polym. Compos. 38 (2017) E433–E442.
[56] Seung Geol Lee, Seung Soon Jang, Jongman Kim, et al., Distribution and diffusion of water in model epoxy molding compound: molecular dynamics simulation approach, TADVP 33 (2010) 333–339.
[57] J. Mijović, H. Zhang, Molecular dynamics simulation study of motions and interactions of water in a polymer network, J. Phys. Chem. B 108 (2004) 2557–2563.
[58] Y.C. Lin, X. Chen, Investigation of moisture diffusion in epoxy system: Experiments and molecular dynamics simulations, Chem. Phys. Lett. 412 (2005) 322–326.
[59] S. Masoumi, H. Valipour, Effects of moisture exposure on the crosslinked epoxy system: an atomistic study, Modell. Simul. Mater. Sci. Eng. 24 (2016) 35011.
[60] S. Pandiyan, J. Krajniak, G. Samaey, et al., A molecular dynamics study of water transport inside an epoxy polymer matrix, Comput. Mater. Sci. 106 (2015) 29–37.
[61] C. Wu, W. Xu, Atomistic simulation study of absorbed water influence on structure and properties of crosslinked epoxy resin, Polymer 48 (2007) 5440–5448.
[62] D. Xin, Q. Han, Investigation of moisture diffusion in cross-linked epoxy moulding compound by molecular dynamics simulation, Mol. Simul. 39 (2013) 322–329.
[63] L. Tam, D. Lau, C. Wu, Understanding interaction and dynamics of water molecules in the epoxy via molecular dynamics simulation, Mol. Simul. (2018) 1–9.
[64] GUHA R. D., O. IDOLOR & L. GRACE. 2019. Molecular Dynamics (MD) Simulation of a Polymer Composite Matrix with Varying Degree of Moisture: Investigation of Secondary Bonding Interactions. In Proceedings of the American Society for Composites—Thirty-Fourth Technical Conference.
[65] LAMMPS: Large-scale Atomic/Molecular Massively Parallel Simulator (https://lammps.sandia.gov/index.html).
[66] W.D. Cornell, P. Cieplak, C.I. Bayly, et al., A second generation force field for the simulation of proteins, nucleic acids, and organic molecules, J. Am. Chem. Soc. 117 (1995) 5179–5197.
[67] W.J. Mortier, K. Van Genechten, J. Gasteiger, Electronegativity equalization: application and parametrization, J. Am. Chem. Soc. 107 (1985) 829–835.
[68] W.L. Jorgensen, J. Chandrasekhar, J.D. Madura, et al., Comparison of simple potential functions for simulating liquid water, J. Chem. Phys. 79 (1983) 926–935.
[69] H. Frank, Theory and molecular models for water, Adv. Chem. Phys. 31 (1975) 1.
[70] J.D. Littell, C.R. Ruggeri, R.K. Goldberg, et al., Measurement of epoxy resin tension, compression, and shear stress–strain curves over a wide range of strain rates using small test specimens, J. Aerospace Eng. 21 (2008) 162–173.
[71] C. Li, A. Strachan, Free volume evolution in the process of epoxy curing and its effect on mechanical properties, Polymer 97 (2016) 456–464.
[72] D. Zhang, K. Li, Y. Li, et al., Characteristics of water absorption in amine-cured epoxy networks: a molecular simulation and experimental study, Soft Matter 14 (2018) 8740–8749.
[73] Y.C. Lin, X. Chen, Moisture sorption–desorption–resorption characteristics and its effect on the mechanical behavior of the epoxy system, Polymer 46 (2005) 11994–12003.
[74] C. Brot, G. Bossis, C. Hesse-Bezot, Molecular dynamics calculation of the dielectric constant, Mol. Phys. 40 (1980) 1053–1072.
[75] O. Gereben, L. Pusztai, On the accurate calculation of the dielectric constant from molecular dynamics simulations: the case of SPC/E and SWM4-DP water, Chem. Phys. Lett. 507 (2011) 80–83.